Hindawi
Computational and Mathematical Methods
Volume 2023, Article ID 4839057, 15 pages
https://doi.org/10.1155/2023/4839057

Research Article

On the Use of Commercial Finite Element Packages for a Dimensionless Solution to a Class of Problems

S. Pashah

Department of Mechanical Engineering, Texas A&M University Texarkana, 7101 University Avenue, BASS 209, Texarkana, TX 75503-0597, USA

Correspondence should be addressed to S. Pashah; spashah@tamut.edu

Received 31 October 2022; Revised 16 April 2023; Accepted 18 April 2023; Published 12 May 2023

Academic Editor: Shadab Alam

Physical laws provide a mathematical description of a physical phenomenon. The mathematical description is generally in the form of differential equations with appropriate initial and boundary conditions, called initial boundary value problems. The dimensionless form of an initial boundary value problem is the first step for the solution to a class of problems. The approach is generally applied for closed-form (or analytical) solutions, whereas practical engineering problems can only be solved numerically. Commercial finite element packages are commonly used for the numerical solution of engineering problems with complexities caused by geometry, loading, and material properties. A numerical solution does not produce a formula; therefore, a completely new solution must be obtained even for minor changes in the data set. A single-dimensionless finite element analysis would solve a class of problems. Literature shows that user-developed finite element codes, not accessible for general use, are generally used for dimensionless finite element solutions. The availability of dimensionless analysis in a commercial finite element package would be very convenient. Commercial packages do not have built-in dimensionless formulations. However, all mainstream packages allow user-implemented formulation through different coding requirements. At least one researcher has used a commercial package for dimensionless analyses without coding. The work presents a guide on alternate implementation methods of dimensionless formulations in commercial packages. A sample case demonstrates the stepwise implementation of a dimensionless formulation without writing a customized finite element code.

1. Introduction

Dimensional analysis and dimensionless parameters are typical for solving thermofluid problems. Dimensional analysis reduces the number of variables of a physical phenomenon by grouping them into dimensionless parameters. The groups are the ratios between the governing variables of the problem; therefore, they provide an intuition of the corresponding physical interpretation of the mathematical solution. In short, it offers a compact presentation, enhanced understanding, and solutions to a class of problems.

Finite element analysis helps solve engineering problems because of the convenience of dealing with complicated geometry, ease in prescribing the loading and boundary conditions, and consideration of anisotropic and nonhomogeneous materials [1–3]. Therefore, commercial finite element packages are prevalent for engineering analyses because the user does not have to derive and implement the mathematical formulation to analyze the engineering problems. Nevertheless, finite element analysis provides the numerical solution of a problem and does not provide a closed-form solution or solve a class of problems. Therefore, a new numerical solution is required for any changes in problem input data. The dimensional finite element analysis of a complex problem would be valid for all similar systems having the same set of dimensionless parameter values. It can be achieved by deriving (i.e., mathematical description) and implementing (through programming code) the dimensionless formulation in a general-purpose software package.

Literature shows that nondimensional finite element analyses are generally implemented through user-developed finite element codes, which are not accessible for general use. In contrast, dimensionless analysis in a commercial finite element package would be accessible to any user. The present work is aimed at evaluating the possibilities and limitations related to a dimensionless solution using a general-purpose commercial software package. A literature review on the state of the art is first presented, followed by deriving and implementing a dimensionless finite element formulation. The present work would serve as a reference and guide to the researchers and engineers on the alternate implementation methods of dimensionless formulations in commercial packages.

2. Literature Review

The methodology used for the literature review is as follows. Google Scholar searches were conducted with the keywords "dimensionless finite element" and "nondimensional finite element." The accessible results were reviewed to evaluate their relevance to the scope of the study. The relevant references of the reviewed papers were the additional source for the literature review. The literature review shows that the application of dimensionless finite element formulation can be categorized as follows:

(1) Fluid dynamics

(2) Dynamic stability of columns

(3) Fracture mechanics of cracked structures

(4) Thermal analysis of extended surfaces

(5) Some discrete applications

2.1. Fluid Dynamics. Although dimensionless parameters are commonly used for analytical solutions, applications of dimensionless finite element analysis are somewhat limited. Apparently, Baker [4] was the first to use the dimensionless finite element formulation in fluid dynamics. He mentioned that "*the finite element concept of solid mechanics is derived for the transient laminar two-dimensional flow of incompressible viscous fluid*." Considering that all commercial finite element packages work with dimensioned quantities, it is interesting that the first fluid dynamics application of the finite element formulation was derived in dimensionless form. The governing dimensionless differential equations for the velocity and pressure distributions were obtained by normalizing them with respect to the characteristic length and velocity parameters. The initial boundary value problem was solved using the Galerkin method of weighted residuals to get the finite element formulation for a triangular element with an nth-order polynomial interpolation function. The formulation was coded into a general-purpose computer program for studying isothermal duct flow in a domain bounded by a nonplanar surface. Winterscheidt and Surana [5, 6], Bell and Surana [7], Edgar and Surana [8], Ling and Surana [9], Musson and Surana [10], Feng and Surana [11], Dalimunthe and Surana [12], and Vijayaraghavan and Surana [13] presented p-version least squares dimensionless finite element formulations for various fluid dynamics problems. The formulations covered the convection-diffusion equation and Newtonian and non-Newtonian isothermal and nonisothermal fluid flow. Bell and Surana also presented a space-time-coupled p-version least square dimensionless formulation for transient, convection-diffusion, and Navier–Stokes equations [14, 15].

The other group of problems is the convection flow in enclosed cavities. Natural convection due to differentially heated side walls in rectangular enclosures corresponds to the cooling of a nuclear reactor, the design of solar collectors, and the simulation of fire spread in buildings [16]. The determination of convection flow in a square cavity can be used to test and validate numerical methods and computer programs to solve viscous flow problems. Therefore, De Vahl Davis et al. [17] proposed the problem of a square cavity as a standard for comparing different numerical methods for fluid flow and convection. The cavity has horizontal adiabatic walls and different-temperature isothermal vertical walls. Taylor and Ijam [18] studied the steady-state free convective flow caused by a temperature gradient within a rectangular enclosed cavity. Their objective was to solve the coupled natural convection problem at high values of Rayleigh numbers using the dimensionless finite element method. Reddy and Satake [19] presented a comparative study of natural convection in enclosures. They used the dimensionless penalty finite element analysis with the stream function vorticity model. Stevens [20] used the Galerkin finite element method with the stream function vorticity formulation to model the steady laminar natural convection for the standard square cavity. Using dimensionless finite element formulation, Misra and Sarkar [16] analyzed the conjugate natural convection in a square enclosure. Oosthuizen [21] presented the dimensionless finite element analysis for convective motion caused by the bottom heating of ice and water in a square enclosure. Barletta et al. [22] used the dimensionless finite element method for studying the combined forced and free flow due to the prescribed heat flux at the walls of a vertical rectangular duct. Basak et al. [23–25] solved the governing mass, momentum, and energy equations. They presented the analyses of natural convection flows in square, trapezoidal, and triangular cavities due to different thermal boundary conditions. They further extended their studies for the cavities filled with a porous medium [26–28]. Rahman et al. [29] derived a dimensionless finite element formulation for the mixed convection due to a heat-conducting horizontal circular cylinder in a rectangular cavity. Mehryan et al. [30] studied free convection in a trapezoidal enclosure divided by a flexible partition using a dimensionless finite element formulation.

Many researchers have studied the convection flow in porous media due to embedded hot plates using the dimensionless finite element method. The engineering applications include geothermal energy technology, petroleum recovery, filtration processes, packed bed reactors, and underground chemical and nuclear waste disposal. Abbas et al. [31] analyzed the effects of thermal dispersion over a flat vertical plate in a porous medium. The governing dimensionless equations were solved using the Galerkin-based FEM method. Palani and Abbas [32] studied the combined effects of radiation and magnetohydrodynamics on the free convection flow of an electricconductive viscous compressible flow past a vertical plate using dimensionless finite element analysis. Rao et al. [33] studied the effects of chemical reactions on the magnetohydrodynamic fluid flow over a flat vertical plate in a porous medium with heat absorption. Sheri et al. [34] presented the heat and mass transfer analysis due to the ramped temperature of an impulsively moving vertical plate using the dimensionless finite element method. Shamshuddin et al. [35] proposed a dimensionless finite element solution of the multiphysical micropolar transport phenomena from an inclined moving plate in a porous media.

Heat transfer and fluid flow studies for flow around cylinders are essential for various engineering applications like heat exchangers and nuclear reactors [36]. Fletcher [37] presented a primitive variable, least-squares dimensionless finite element formulation for inviscid, compressible flow. The unique feature was that the formulation was derived from groups of variables rather than single variables. Velocity, density, and pressure were nondimensionalized with respect to characteristic velocity and density values. The formulation was used for studying the inviscid compressible flow over cylindrical and elliptical cylinders and aerofoils. Dhaubhadel et al. [36, 38] studied the laminar incompressible flow across the staggered and inline bundles of cylinders. They used the penalty-dimensionless finite element model for solving the two-dimensional steady-state Navier-Stokes and energy equations. Apparently, it was the first application of the dimensionless finite element formulation for solving the flow across the bundle of cylinders [36]. Mahmood et al. [39] studied the laminar flow of Bingham fluid past a 2-D circular cylinder using dimensionless finite element formulation. Bingham fluids can sustain nonzero shear stress, and flow occurs when the applied shear stress is more than a limiting shear stress value [39].

Researchers have studied convection flow in enclosures, Couette flow, natural convection over a vertical flat plate embedded in a porous medium, and flow across cylinders using dimensionless finite element analysis. Indeed, the closed-form solution of all these problems is obtained by solving dimensionless governing differential equations analytically. Therefore, a dimensionless finite element solution is considered when an analytical solution is either challenging or impossible.

2.2. Dynamic Stability of Columns. Multiple researchers have studied the dynamic structural stability of Beck's column using dimensionless finite element analysis. Beck's column is a cantilever subjected to a tangential follower load at the free end [40], such as those caused by rocket and jet engines. In a review paper, Langthjem and Sugiyama [40] presented the dimensionless boundary value problem related to Beck's column's basic linear dynamic and stability. They discussed the semianalytical solutions available in the literature for the columns with uniform mass and stiffness distribution. In contrast, a discretization method is required for nonuniform cross-sections or distributed loads [40]. Therefore, the dimensionless finite element method has been used to analyze Beck's column.

Apparently, Mote Jr. [41] and Barsoum [42] were the first to apply finite element solutions almost simultaneously for Beck's column. Using an adjoint system, Prasad and Herrmann [43] solved the dimensionless boundary value problem related to nonconservative stability problems. They concluded that the adjoint variational method is formally like the Galerkin method under certain conditions. Rao et al. [44, 45] obtained the governing differential equation for the lateral motion of a cantilevered column with a tangential load and obtained the solution using finite element formulation based on the Galerkin method. The formulation was then further extended for the damping effects [46]. Rao and Raju [47] used the Galerkin finite element formulation to solve the nondimensional governing equations for conducting post-buckling analysis of uniform cantilever columns. Ryu et al. [48, 49] studied the dynamic stability of Timoshenko columns with a rigid body at the tip and subjected to subtangential forces. They obtained the dimensionless finite element formulation by using extended Hamilton's principle. Langthjem and Sugiyama [50, 51] presented the stability optimization of undamped cantilevered columns subjected to the simultaneous action of a conservative and a nonconservative load at their free ends. They solved the dimensionless optimization problem using the finite element method and sequential linear optimization. Lee et al. [52, 53] investigated the dynamic stability of the damped Beck's column on an elastic foundation under concentrated and linearly distributed follower force using dimensionless finite element formulation based on the extended Hamilton's principle. Goyal and Kapania [54] derived a 5-node, 21-degree-of-freedom dimensionless finite element based on the first-order shear deformation theory to analyze laminated composites under dynamic and static loads. The closed-form element tangent stiffness and mass matrices were derived using a dynamic version of the principle of virtual work. The dimensionless formulation was validated against an analytical solution for natural frequencies for isotropic and laminated beams with different boundary conditions. The formulation is then used for studying laminated beams' stability under subtangential loading and a combination of conservative and nonconservative tangential follower loads [55]. Viola and Marzani [56] performed a dimensionless finite element analysis of the dynamic stability of restrained cracked beams. The beams were subjected to triangularly distributed subtangential conservative and nonconservative forces. Another approach some researchers use is conducting the conventional finite element analysis and then converting the results into the nondimensional form [57–59].

Most formulations were used for solving the dimensionless governing equations of a particular problem, except for the Goyal-Kapania element for composite laminates. They first presented a general-purpose one-dimensional finite element formulation for composite laminate structures (like beams and columns) under static and dynamic loadings. The formulation was then applied to study the beams' dynamic stability under nonconservative loads. The dynamic stability of columns and beams is studied through dimensionless analysis. Therefore, researchers have used dimensionless finite element analyses for problems that are too complicated for an analytical solution.

2.3. Fracture Mechanics of Cracked Structures. Fracture mechanics use stress intensity factors to study stresses at the crack tip. The stress intensity factors are not dimensionless parameters. However, using charts with dimensionless parameters for stress estimation at the crack tip is prevalent. Therefore, some researchers have used dimensionless finite element analysis to analyze cracked structures.

Sanz et al. [60] used dimensionless finite element results to analyze the applicability of the Brazilian test to determine the tensile strength of ultra-high-performance fiber-reinforced concrete (UHPFRC). They conducted finite element simulations through a commercial package COFE (Continuum Oriented Finite Element). Fang and Charalambides [61] studied a cantilever beam with an embedded sharp crack using a dimensionless finite element analysis and reported the mode I and II stress intensity factors. Bogdański and Trajer [62] introduced a dimensionless finite element model to solve a class of rolling contact fatigue crack problems.

None of the studies presented any dimensionless finite element formulation, only the governing dimensionless parameters. The dimensioned parameters corresponded to the desired values of governing dimensionless parameters. Therefore, the results of finite element simulations were valid for the class of problems.

2.4. Heat Transfer from Extended Surfaces. Extended surfaces (or fins) increase heat transfer between a prime surface and its' surrounding environment by providing additional surface area for convection. Closed-form solutions are available for fin efficiency and temperature distribution for various fin geometry and operating conditions. The complexity of a problem depends on the geometry, material, and operating conditions. For instance, if the fin has a variable cross-section with a coating layer, the analytical solution can become challenging, and the finite element method would be the suitable choice.

Pashah et al. [63–65] derived a general finite element formulation for conduction in orthotropic material with convection boundary conditions. They extended the formulation to account for dehumidifying conditions (i.e., both latent and sensible heat transfer from the fins) in references [66, 67]. They used the developed finite elements to study the fin problems for which analytical solutions are unavailable in the literature, i.e., variable thickness composite pin, plane, and annular fins, with contact resistance. However, they only used the general finite element formulation to analyze extended surfaces and did not consider any other applications.

2.5. Some Discrete Applications. Most of the dimensionless finite element applications fall under a group of problems. However, some researchers have applied it to discrete applications. Endahl [68] studied the Hertz contact problem for elastoplastic deformation using dimensionless finite element analysis. Basak et al. [69] used the Galerkin method to solve the dimensionless governing equations to estimate the temperature distribution in a honeybee swarm. Fredriksson and Gudmundson [70] analyzed a thin film's biaxial strain and pure shear through the dimensionless finite element method. Abbas and Youssef [71] presented a transient dimensionless finite element analysis for a thermoelastic solid. Toit and Pretorius [72] derived a dimensionless finite element formulation for studying steady-state heat transfer in a spherical domain.

2.6. Conclusion of the Presented Literature Review. The literature review demonstrates that the most frequent applications relate to fluid dynamics and heat transfer problems because dimensionless solutions are prevalent in these fields. Similarly, the applications for structural analysis focus on the problems studied through dimensionless closed-form solutions. Therefore, a dimensionless finite element solution replaces an impossible or challenging dimensionless closed-form solution. The implementation is mostly through user-programmed codes, with a few through commercial software. It is because commercial packages use the dimensioned form of the governing equations. The limitation of user-defined codes is twofold. It requires a considerable amount of programming effort to write a complete finite element code. Also, the code may not be easily accessible to others, and its application becomes limited to developers only. Commercial finite element software can usually incorporate customized formulations as user-defined elements. The benefit of using such a feature would be the ease of implementation because only the formulation needs to be programmed while using the commercial software's built-in pre- and postprocessing capabilities. Moreover, any user can use the code for different applications.

The following section investigates the possibilities and challenges of implementing a dimensionless finite element formulation in a general-purpose finite element analysis package. Therefore, the derivation of a basic finite element formulation in conventional (i.e., dimensioned) and dimensionless form is first presented. The objective is to identify the differences between the two formulations from an implementation point of view.

3. Conventional and Dimensionless Finite Element Formulation for Heat Transfer

A finite element solution provides a numerical solution to an initial boundary value problem (i.e., a differential equation with initial and boundary conditions). The finite element formulation consists of a set of equations called element equations. The element equations are obtained by converting the strong form to a weak form, followed by its minimization. The strong form is the actual governing differential equation with the specified initial and boundary conditions (i.e., initial boundary value problem). In contrast, the weak form is an equivalent integral form that is more convenient for obtaining the approximate numerical solution in the form of element equations. The strong form states the conditions that must be met at every point of the studied domain, whereas the weak form states the requirements that must be met only in an average or integral sense. The derivation process is identical for both conventional and dimensionless formulations. The following section presents the traditional and dimensionless finite element formulations for steady-state heat transfer problems.

3.1. Strong Form: Differential Equation with Boundary Conditions. The boundary value problem for steady-state heat conduction in a three-dimensional orthotropic space without internal heat generation is described through the following differential equation [73]:

$$k_x \frac{\partial^2 T}{\partial x^2} + k_y \frac{\partial^2 T}{\partial y^2} + k_z \frac{\partial^2 T}{\partial z^2} = 0, \quad (1)$$

and the associated boundary conditions

$$\begin{gathered} T = T_b \quad \text{on surface } S_1, \\ k_x \frac{\partial T}{\partial x}\hat{l} + k_y \frac{\partial T}{\partial y}\hat{m} + k_z \frac{\partial T}{\partial z}\hat{n} + q = 0 \quad \text{on surface } S_2, \\ k_x \frac{\partial T}{\partial x}\hat{l} + k_y \frac{\partial T}{\partial y}\hat{m} + k_z \frac{\partial T}{\partial z}\hat{n} + h(T - T_\infty) = 0 \quad \text{on surface } S_3, \end{gathered} \quad (2)$$

where k_x, k_y, and k_z are the orthotropic thermal conductivities, T_b and T_∞ are the surface and surrounding temperatures, q is the prescribed heat flux, h is the convective heat transfer coefficient, $\hat{l}$, $\hat{m}$, and $\hat{n}$ are the unit vectors, whereas S_1, S_2, and S_3 are the surfaces corresponding to temperature, heat flux, and convective boundary conditions because these conditions cannot coexist.

3.2. Weak Form: The Variational Principle. The variational principle provides the weak integral form of the continuum problem through a scalar quantity (called functional Π) given by [74]

$$\Pi = \mathrm{U} + \Omega_q + \Omega_h. \quad (3)$$

The three terms correspond to internal energy (U), heat convection (Ω_h), and heat conduction (Ω_q), are given by [74]

$$\begin{aligned} U &= \frac{1}{2}\iiint_V \left[k_x\left(\frac{\partial T}{\partial x}\right)^2 + k_y\left(\frac{\partial T}{\partial y}\right)^2 + k_z\left(\frac{\partial T}{\partial z}\right)^2\right] dV, \\ \Omega_q &= -\iint_{S_2} qT\,dS, \\ \Omega_h &= \frac{1}{2}\iint_{S_3} h(T - T_\infty)^2 dS. \end{aligned} \quad (4)$$

Therefore, equation (3) reduces to

$$\begin{aligned} \Pi = \frac{1}{2}\iiint_V &\left[k_x\left(\frac{\partial T}{\partial x}\right)^2 + k_y\left(\frac{\partial T}{\partial y}\right)^2 + k_z\left(\frac{\partial T}{\partial z}\right)^2\right] \\ &\cdot dV - \iint_{S_2} qT\,dS + \frac{1}{2}\iint_{S_3} h(T - T_\infty)^2 dS. \end{aligned} \quad (5)$$

3.3. Finite Element Formulation. The textbooks contain detailed derivation steps for the conventional finite element formulation of a heat transfer problem. Therefore, the result is reported here for completeness purposes. The minimization of the functional with respect to the temperature provides the finite element formulation, which can be expressed in the following matrix form [74]:

$$\begin{aligned} &\left[\iiint_V [\mathbf{B}]^T[\mathbf{D}][\mathbf{B}]\,dV + \iint_{S_3} h\,[\mathbf{N}]^T[\mathbf{N}]dS\right]\{\mathbf{T}\} \\ &\quad = \iint_{S_2} q[\mathbf{N}]^T\,dS + \iint_{S_3} hT_\infty[\mathbf{N}]^T dS. \end{aligned} \quad (6)$$

The superscript T represents the transpose of a matrix. $[\mathbf{D}]$ is the material property matrix, whereas $[\mathbf{N}]$ and $[\mathbf{B}]$ are shape function and strain matrices, respectively. The order of these matrices is governed by element shape, number of nodes, and geometry.

3.4. Dimensionless Finite Element Formulation. The following nondimensional parameters are defined

$$\theta = \frac{T}{T_\infty} \quad \bar{q} = \frac{q}{hT_\infty} \quad \bar{x} = \frac{x}{L_x} \quad \bar{y} = \frac{y}{L_y} \quad \bar{z} = \frac{z}{L_z}, \quad (7)$$

where θ is the nondimensional temperature, $\bar{q}$ is the dimensionless heat flux, $\bar{x}$, $\bar{y}$, and $\bar{z}$ are dimensionless coordinates, L_x, L_y, and L_z are the characteristic lengths for normalizing dimensions in x, y, and z directions, respectively.

The dimensionless strong form becomes

$$\frac{1}{\mathrm{Bix}}\frac{\partial^2\theta}{\partial\bar{x}^2} + \frac{L_x}{L_y}\frac{1}{\mathrm{Biy}}\frac{\partial^2\theta}{\partial\bar{y}^2} + \frac{L_x}{L_z}\frac{1}{\mathrm{Biz}}\frac{\partial^2\theta}{\partial\bar{z}^2} = 0, \quad (8)$$

with the following boundary conditions

$$\theta = \theta_b \quad \text{on surface } \bar{S}_1, \quad (9)$$

$$\frac{1}{\mathrm{Bix}}\frac{\partial\theta}{\partial\bar{x}}\hat{l} + \frac{1}{\mathrm{Biy}}\frac{\partial\theta}{\partial\bar{y}}\hat{m} + \frac{1}{\mathrm{Biz}}\frac{\partial\theta}{\partial\bar{z}}\hat{n} + \bar{q} = 0 \quad \text{on surface } \bar{S}_2, \quad (10)$$

$$\frac{1}{\mathrm{Bix}}\frac{\partial\theta}{\partial\bar{x}}\hat{l} + \frac{1}{\mathrm{Biy}}\frac{\partial\theta}{\partial\bar{y}}\hat{m} + \frac{1}{\mathrm{Biz}}\frac{\partial\theta}{\partial\bar{z}}\hat{n} + (\theta - 1) = 0 \quad \text{on surface } \bar{S}_3, \quad (11)$$

where $\mathrm{Bix} = hL_x/k_x$, $\mathrm{Biy} = hL_y/k_y$, and $\mathrm{Biz} = hL_z/k_z$ are the Biot numbers, whereas $\bar{S}_1$, $\bar{S}_2$, and $\bar{S}_3$ are the dimensionless surface areas, as explained in the appendix. Substituting the dimensionless parameters in functional (cf. equation (5)) provides the dimensionless form of functional Π as follows (Detailed step by step calculation is given in the appendix.):

$$\bar{\Pi} = \frac{1}{2}\iiint_{\bar{V}} \left[\frac{1}{\mathrm{Bix}} \left(\frac{\partial \theta}{\partial \bar{x}} \right)^2 + \frac{L_x}{L_y} \frac{1}{\mathrm{Biy}} \left(\frac{\partial \theta}{\partial \bar{y}} \right)^2 + \frac{L_x}{L_z} \frac{1}{\mathrm{Biz}} \left(\frac{\partial \theta}{\partial \bar{z}} \right)^2 \right] \cdot d\bar{V} - \iint_{\bar{S}_2} \bar{q}\theta d\bar{S} + \frac{1}{2}\iint_{\bar{S}_3} (\theta - 1)^2 d\bar{S}. \tag{12}$$

Minimizing $\bar{\Pi}$ with respect to dimensionless temperature provides

$$\left[\iint_V [\bar{\mathbf{B}}]^T [\bar{\mathbf{D}}] [\bar{\mathbf{B}}] d\bar{V} + \iint_{S_3} [\bar{\mathbf{N}}]^T [\bar{\mathbf{N}}] d\bar{S} \right] \{\boldsymbol{\theta}\} = \iint_{S_2} [\bar{\mathbf{N}}]^T q d\bar{S} + \iint_{S_3} [\bar{\mathbf{N}}]^T d\bar{S}. \tag{13}$$

On comparing the dimensionless formulation with the conventional formulation (cf. equation (7)), it is noted that the dimensionless formulation has the same dimensionless matrices (i.e., $[\bar{\mathbf{B}}]$,$[\bar{\mathbf{D}}]$, and $[\bar{\mathbf{N}}]$) that exist in a conventional finite element formulation given by equation (6). However, the elements of these matrices are dimensionless groups rather than individual variables, as described in the following.

3.5. Validity of Dimensionless Solution for Similar System. Similar systems must have the same set of dimensionless parameter values. The formulation has only two dimensionless parameters corresponding to the studied domain. q is the dimensionless specified heat flux, whereas matrix $[\bar{\mathbf{D}}]$ contains two similarity groups, i.e., the Biot number and the aspect ratios. The same parameters appear in the dimensionless strong form (cf. (8) and (9)). Therefore, the finite element formulation has not added any additional similarity requirements for the domain of study, and it would be valid for a class of problems having the same set of values for q and $[\bar{\mathbf{D}}]$.

Next, the possibility of implementing the derived dimensionless finite element formulation (c.f. equation (13)) in a commercial package is investigated.

4. Implementation of a Dimensionless Finite Element Formulation in a Commercial Package

Commercial finite element packages are vital for engineering analysis because they ease dealing with arbitrary geometry, material, and loading conditions without going through a tedious and challenging implementation process of mathematical derivation followed by its implementation through computer programming. A brief overview of the finite element analysis process would help understand the possibilities and implementation challenges of a dimensionless formulation in a commercial package.

4.1. Steps of a Finite Element Analysis in a Commercial Package. The finite element analysis has three phases: preprocessing, solution, and postprocessing.

Preprocessing corresponds to the problem description in a commercial package. It defines the geometry, material, loads, and initial and boundary conditions. The defined geometry is also divided into subdomains called "finite elements." The process is called discretization, and the collection of elements is called a finite element mesh. An appropriate element type from the built-in element library is selected according to the physics of the problem (e.g., heat transfer or stress analysis). An option for user-defined element types must be available to implement a dimensionless formulation in a commercial package. Therefore, implementing a dimensionless form of the available dimensioned formulation would be possible only if the package allows the user to modify any of the strong, weak, or element equations coded and implemented by the developer.

The second step is the solution to the defined problem. The program code takes care of the solution process in commercial software. The end user does not have any direct interaction with this step apart from selecting solution options. Indeed, this is the main reason for using a commercial package because it automatically solves a system of element equations corresponding to the entire mesh under specified loads, initial, and boundary conditions.

The last step is post-processing. It is the visualization of estimated results in contour plots, tabulated data, and graphical form. This handy feature helps users analyze the results through various practical and convenient data analysis tools.

Therefore, the difference between a conventional and dimensionless finite element analysis would be at the preprocessing level only. The problem description would need to be in terms of governing dimensionless parameters rather than dimensioned ones. The most challenging part would be to include the dimensionless element as a user-defined element in the existing element library of commercial software. In the next section, the available options for user-defined elements in the commercial finite element packages are first reviewed, followed by a discussion of the implementation possibility for a user-defined dimensionless finite element formulation.

4.2. Existing User-Defined Element Formulation in Commercial Packages. A finite element package has a built-in element library to select elements according to the physics of the problem to be solved. Many commercial packages provide the option to implement user-defined formulations. In the following, the available options for user-defined element formulations in commercial software packages are reviewed. It would help identify the possibilities of using strong, weak, or element equations.

Jeffers [75] presented a heat transfer element for modeling the 3D thermal response in plates and shells exposed to nonuniform heating. The formulation was obtained as element equations and implemented in ABAQUS [76] as a user-defined element. In ABAQUS, a user-defined element can be used by providing the element matrices (as direct input or in the form of a data file) [77] or through a user subroutine that performs all calculations for the element matrices [78]. Therefore, ABAQUS implements element equations rather than strong or weak forms. Brouwer et al. [79] implemented user-defined elements in the commercial software ANSYS [80] for 2D multiphysics modeling of superconducting magnets. The approach was based on modifying and coupling the existing elements to incorporate customized features in the finite element formulation. The implementation was through coding, which defines element properties and builds the finite element matrices. The code is then compiled as an ANSYS executable that allows selecting the user-defined element the same way as an ANSYS built-in element [79].

The implementations mentioned above are for the conventional (i.e., dimensioned) user-defined elements in commercial software. Next, evaluating if the dimensionless formulation has been implemented in commercial software is interesting. Reeve et al. [81] studied natural convection in an annular cavity. They used the finite element code FIDAP to solve the dimensionless axisymmetric Navier-Stokes equations [82]. However, it is unclear if they implemented a strong form or element equations because implementation details were not discussed. Khanafer and Aithal [83] obtained the dimensionless form of the boundary value problem to study the mixed convection flow and heat transfer characteristics in a lid-driven cavity with a circular body inside. They did not provide the element equations but a general description of getting the finite element formulation based on the Galerkin method with the implementation in commercial software ADINA [84]. The mesh and the contour plots from the simulation results were presented in dimensionless form. ADINA allows a user-defined element by entering the element matrices or by coding in an ADINA subroutine to calculate the element matrices and vectors [85]. The two examples imply that implementing a dimensionless formulation is possible in commercial software.

The implementations above (dimensioned and dimensionless) are through element equations. Deriving element equations and programming them as source code is the most challenging part of implementing a user-defined finite element formulation. Implementing the strong form would be the most convenient as that would neither require deriving element equations nor programming them. Dillon et al. [86] presented the dimensioned and dimensionless solution for natural convection in a tall cavity using COMSOL [87]. The motivation for their study was that most experimental correlations for CFD and heat transfer problems are expressed in dimensionless groups, whereas the commercial codes are in dimensioned form. Therefore, a dimensioned solution must be compared against a benchmark dimensionless solution or be calibrated with a key dimensionless parameter. The other consideration was that a single strong form might be converted into alternate dimensionless forms, depending on the choice of the nondimensionalization scheme. They presented three alternate sets of governing dimensionless parameters for the dimensionless strong forms. They obtained the dimensionless solutions without deriving the dimensionless finite element formulations. Getting alternate dimensionless solutions without deriving and

Table 1: Comparison of parameters for dimensioned and dimensionless formulations.

Dimensioned parameter	Dimensionless parameter	Definition
x (m)	$\bar{x}$	$\frac{x}{L_x}$
y (m)	$\bar{y}$	$\frac{y}{L_y}$
z (m)	$\bar{z}$	$\frac{z}{L_z}$
T (°C)	θ	$\frac{T}{T_\infty}$
q (W/m^2)	$\bar{q}$	$\frac{q}{hT_\infty}$
k_x (W/m•K)	$\frac{1}{\text{Bix}}$	$\frac{k_x}{hL_x}$
k_y (W/m•K)	$\left(\frac{L_x}{L_y}\right)\frac{1}{\text{Biy}}$	$\left(\frac{L_x}{L_y}\right)\frac{k_y}{hL_y}$
k_z(W/m•K)	$\left(\frac{L_x}{L_z}\right)\frac{1}{\text{Biz}}$	$\left(\frac{L_x}{L_z}\right)\frac{k_z}{hL_z}$
h (W/m^2•K)	1	–
T_∞ (°C)	1	–
Q (W)	$\bar{Q}$	$\frac{Q}{hT_\infty L_y L_Z}$

implementing the corresponding finite element equations is highly convenient. Indeed, COMSOL allows the user to define the strong form and then convert it into the weak form, followed by its numerical solution using the finite element method [88]. They validated their approach by considering Reeve et al.'s dimensionless finite element solution [81] as a benchmark. They also obtained the dimensioned (conventional) finite element solution in COMSOL that was in excellent agreement with the corresponding dimensionless finite element solutions.

4.3. Implementation Options for the Heat Transfer Dimensionless Finite Element Formulation. The preceding section showed that most commercial software allows user-defined formulation through element equations, except for one software that enables implementation through strong and weak formulation. Therefore, the presented heat transfer formulation can also be implemented in one of three ways, depending on the choice of commercial software. The most straightforward method would be the comparison method used by Dillon et al. [86], as follows. The presented formulation is the dimensionless form of a standard heat transfer formulation already available in any commercial software. Therefore, the implementation would be straightforward by identifying the dimensionless counterpart of each dimensioned parameter. The comparison of the two types of governing parameters is presented in Table 1.

Therefore, replacing dimensioned parameters with their counterparts in a commercial package should provide a dimensionless solution. The cylindrical spine studied by

Bahadur and Bar-Cohen [89] and Zubair et al. [90] is considered the benchmark solution to verify this approach. The schematic of the fin is presented in Figure 1, having the following governing parameters:

Geometry: $R = 0.45$ cm, $L = 5$ cm

Material: $k_z = 20\,\mathrm{W/m-K}$ with multiple k_r values

Loading: fin base temperature $T_b = 95^\circ\mathrm{C}$

Boundary condition: convective fin tip with $T_\infty = 45^\circ\mathrm{C}$ and multiple h values

For the finite element analysis, the presented three-dimensional formulation (cf. equation (13)) can be easily converted to the axisymmetric case, and the details can be found in [63]. The characteristic lengths are taken to be $L_z = L_r = L = 5\,\mathrm{cm}$. The benefit of considering both characteristic lengths equal to the fin length is that the aspect ratio of the dimensionless mesh would be the same as the actual fin aspect ratio, with a unit dimensionless fin length, whereas taking $L_z = L$ and $L_r = R$ would result in the dimensionless fin geometry as a unit square [63]. The dimensioned and dimensionless finite element analyses use the same element type and mesh size. The mesh size is chosen after checking the convergence of the results for total heat loss. The finite element results for total heat loss are compared with the reference closed-form solutions in Table 2.

The dimensionless heat loss $\bar{Q}$ is reported with multiple decimal places to avoid the round-off error while converting it to the corresponding dimensioned value Q_{NDFEA}, as follows:

$$Q_{\mathrm{NDFEA}} = (hT_\infty L_r L_z)\bar{Q}. \tag{14}$$

It is evident that the dimensioned value Q_{NDFEA} (based on the dimensionless heat loss $\bar{Q}$) agrees well with the conventional finite element analysis result Q_{FEA}.

Indeed, the comparison method works because the dimensionless formulation (c.f. equation (13)) has the same number and arrangement of matrices as the dimensioned form (c.f. equation (6)). Moreover, all the coefficients are constant values, and material properties do not depend on temperature. Depending on the options available for user input data in a commercial package, a dimensionless solution based on the comparison method might be challenging or incompatible.

5. Discussion

The preceding section shows that the comparison method's dimensionless solution was relatively straightforward for simple geometry and a linear steady-state problem. The numerical methods are, however, necessary for nonlinear problems and complicated geometries. For example, an application to Navier-Stokes (a parabolic partial differential equation) would be interesting in the case of fluid dynamics. This section discusses the probability of obtaining a dimensionless finite element solution through commercial packages for nonlinear problems and complicated geometries.

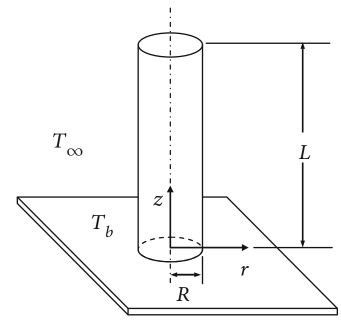

Figure 1: A cylindrical pin fin.

5.1. Application to Nonlinear Problems. As mentioned earlier, Baker [4] was the first to use the dimensionless finite element method based on the Navier-Stokes equation for viscous, incompressible fluid dynamics. He then extended the dimensionless finite element formulation for the elliptic partial differential equation description of the Navier-Stokes system [91]. The complete details of the dimensionless nonlinear finite element formulation were reported; however, it was implemented through a user-written code called COMOC.

Dillon et al. [86] studied buoyancy-driven transient flow in a tall cavity. It is modeled through a coupled fluid motion system governed by Navier-Stokes and the convection and conduction heat transfer. They employed the comparison method to obtain the nonlinear transient dimensionless solution of the problem in the commercial finite element package COMSOL and validated it through a known solution. It is possible to get the dimensionless solution of a nonlinear transient problem using a commercial package.

5.2. Application to Complicated Geometries. The finite element method can deal with complicated geometry without considerable difficulties. The challenge is usually related to the singularity at sharp corners, and it can be addressed by mesh refinement or slight modification of the geometry. However, once the geometry is meshed, the solution by a dimensionless solution would mainly depend on how a nondimensional system is defined. Indeed, two different dimensionless schemes of the same system should not change the results of the system. However, depending on the scale of each dimensionless scheme, the numerical rounding may influence the accuracy of the results [86]. It may be addressed by modeling considerations according to the dimensionless scheme. To demonstrate this, let us reconsider the nominal case of the pin fin study (cf. Figure 1). The geometric parameters related to the dimensionless scheme are $L_z = L_r = L = 5\,\mathrm{cm}$. The corresponding uniform meshes for the dimensioned and dimensionless finite element model are shown in Figures 2(a) and 2(b). For demonstration purposes, the shown meshes are not for the converged results presented in Table 2, but only for an initial mesh with square-shape elements. An alternate dimensionless scheme would be $L_z = L = 5\,\mathrm{cm}$ and $L_r = R = 0.45\,\mathrm{cm}$. This leads to a square, dimensionless geometry for the fin

Table 2: Comparison of dimensionless and conventional FEA results with the ones available in the literature.

Case	$Q_{\text{Raj}}(\text{W})$	$Q_{\text{Zub}}(\text{W})$	Dimensionless FEA $\bar{Q}$	Dimensionless FEA $Q_{\text{NDFEA}}(\text{W})$	$Q_{\text{FEA}}(\text{W})$
$h = 100\ \text{W/m}^2\text{K}$, $k_r = 0.5k_z$	2.94	2.94	0.26132	2.94	2.94
$h = 500\ \text{W/m}^2\text{K}$, $k_r = k_z$	6.59	6.55	0.11781	6.627	6.627
$h = 1000\ \text{W/m}^2\text{K}$, $k_r = 2k_z$	9.35	9.36	0.08331	9.372	9.372
$h = 5000\ \text{W/m}^2\text{K}$, $k_r = 4k_z$	20.66	20.64	0.036708	20.648	20.648

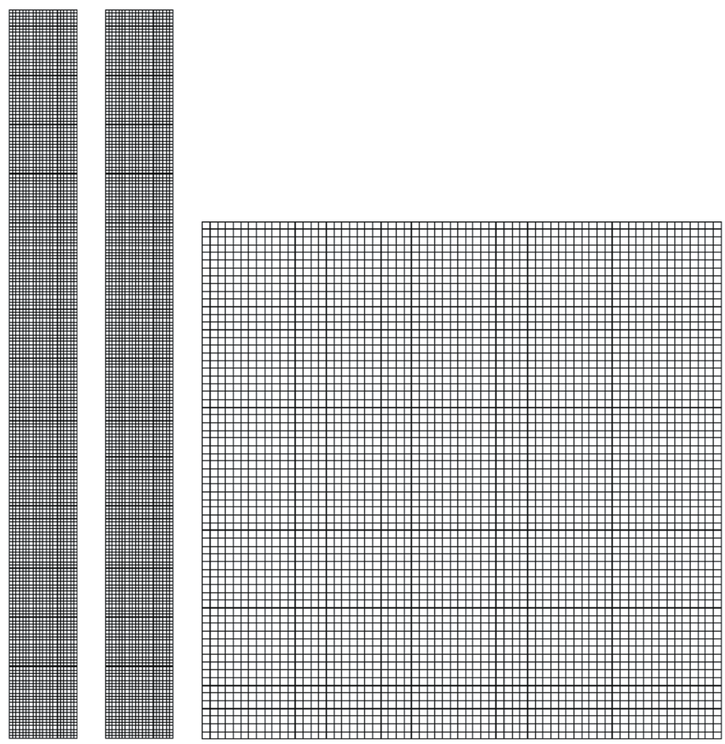

(a) (b) (c)

Figure 2: Uniform meshes for the pin fin of the nominal case of study. (a) Dimensioned model. (b) Dimensionless model with $L_z = L_r = L$. (c) Dimensionless model with $L_z = L$ and $L_r = R$.

as shown in Figure 2(c). The meshing details and results for heat loss are summarized in Table 3. The dimensioned values in parentheses for heat loss are obtained using equation (14).

It can be noted that the first dimensionless scheme is better than the second one because it preserves the aspect ratio of the actual geometry. Therefore, it has the identical mesh and heat loss value for the dimensioned model. On the other hand, the second dimensionless scheme provides an overestimated value for heat loss despite having a slightly higher number of elements than the other models. The dimensionless scheme has changed the rectangular aspect ratio to a dimensionless square domain. Therefore, a square-shaped elements mesh for the dimensionless square domain (cf. Figure 2(c)) would correspond to a rectangular-shaped elements mesh for the dimensioned model, as shown in Figure 3. The mesh is overly refined in the radial direction (that makes the mesh of the entire fin appear as filled black in Figure 3(a)).

On the contrary, the mesh is very coarse in the longitudinal direction (as shown in the zoom views of the fin top and bottom portions in Figure 3(b)). The temperature gradient in the longitudinal direction would be much larger than the radial direction, and a coarse mesh in the longitudinal direction near the fin base cannot capture the large thermal gradients. Therefore, a fine mesh must be used near the fin base in the longitudinal direction, and a coarse mesh can be used near the fin tip. The nonuniform meshes that provided the converged results (cf. Table 2) are shown in Figures 4(a) and 4(b). The meshes for the rectangular domains have the same number of elements as before (i.e., Figure 2). The only difference is that the element size only varies in the longitudinal direction (mesh size in the radial direction is the same as before). Mapping the refined mesh of the dimensioned model (i.e., $20 \times 222 = 4{,}440$ elements) on the square dimensionless domain, as shown in Figure 4(c), results in a dimensionless heat loss $\bar{Q} = 0.40786$ (i.e., $Q_{\text{NDFEA}} = 20.648\ \text{W}$) which is in excellent

Table 3: Comparison of finite element results for dimensioned with two different dimensionless models for the nominal case of pin fin study ($h = 5000\ \mathrm{W/m^2K}$, $k_r = 4k_z$).

Case	Number of elements in r and z directions	Geometric size		Heat loss
		Radial	Longitudinal	
Dimensioned	$20 \times 222 = 4{,}440$	0.45 cm	5 cm	20.665 W
Dimensionless 1	$20 \times 222 = 4{,}440$	0.09	1	0.036738 (20.665 W)
Dimensionless 2	$67 \times 67 = 4{,}489$	1	1	0.41177 (20.846 W)

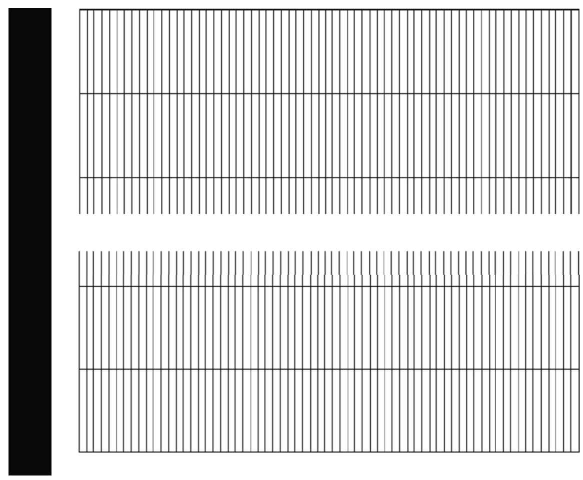

(a) (b)

Figure 3: Mapping of square domain dimensionless uniform mesh on the dimensioned model. (a) Mesh for the entire fin. (b) Zoom view of fin top and bottom portions to show the mesh details.

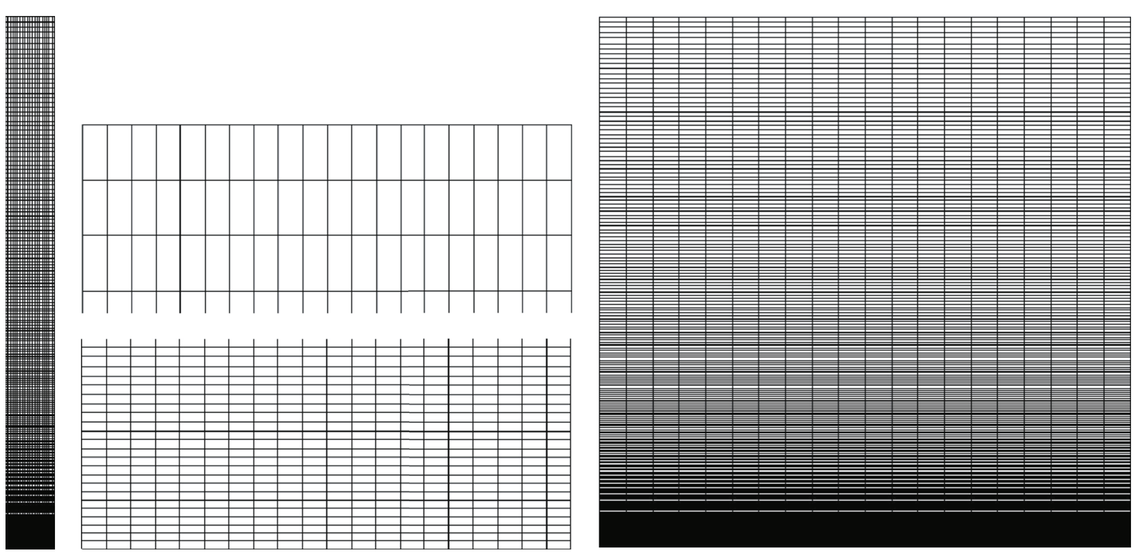

(a) (b) (c)

Figure 4: Nonuniform meshes for the pin fin of the nominal case of study. (a) Dimensioned and dimensionless model with $L_z = L_r = L$. (b) Zoom view of rectangular domain fin top and bottom portions to show the mesh variation details. (c) Dimensionless model with $L_z = L$ and $L_r = R$.

agreement with the dimensioned results reported in Table 2. It demonstrates that modeling considerations must be per the dimensionless scheme to attain the desired level of accuracy of the result values.

5.3. Findings of the Present Study. The present study finds that many researchers have used finite element analysis to solve dimensionless initial-boundary-value problems. Most researchers have focused on solving their specific problems through user-developed codes. The reason might be that the commercial packages were not flexible for implementing customized formulations. However, the latest commercial packages provide users with more flexibility to implement customized formulations with minimal or no coding efforts. Therefore, the present study makes the following contributions:

(1) It provides a general overview of the state of the art from the first applications to the recent ones

(2) It demonstrates the implementation of a dimensionless formulation without writing a code

(3) It summarizes different ways of a dimensionless analysis using a commercial package. It would serve as a reference and guide for the researchers and engineers

6. Concluding Remarks

The implementation of dimensionless finite element analysis in commercial packages is mainly through user-written codes at the element equation level. In contrast, if commercial software has the option to describe the strong and weak forms, then the coding efforts would be relatively insignificant. Commercial packages have built-in formulations in dimensioned forms. The dimensionless solution of a built-in formulation can be obtained by a "comparison method" that does not require any coding efforts. The method involves getting the dimensionless counterpart to each dimensioned parameter. A finite element analysis based on the identified dimensionless parameters provides a dimensionless solution. Different dimensionless schemes may require additional modeling considerations to attain the same accuracy level of the results.

Therefore, it is possible to use the commercial finite element packages for the dimensionless solution in the following three ways:

(1) Implementation as user-defined dimensionless element equations

(2) Implementing dimensionless strong (or weak) form

(3) Comparison of the dimensionless form with the built-in dimensioned formulation

Appendix

Derivation Steps for Dimensionless Finite Element Formulation

Substitution of dimensionless variables in the functional gives

$$\frac{\Pi}{hT_\infty^2} = \frac{1}{2}\iiint_V \left[\frac{1}{L_x}\frac{1}{\mathrm{Bix}}\left(\frac{\partial\theta}{\partial\bar{x}}\right)^2 + \frac{1}{L_y}\frac{1}{\mathrm{Biy}}\left(\frac{\partial\theta}{\partial\bar{y}}\right)^2 + \frac{1}{L_z}\frac{1}{\mathrm{Biz}}\left(\frac{\partial\theta}{\partial\bar{z}}\right)^2\right] \cdot dV - \iint_{S_2}\bar{q}\theta dS + \frac{1}{2}\iint_{S_3}(\theta-1)^2 dS. \quad (A.1)$$

Which can be converted into dimensionless form by dividing by L_yL_z as follows:

$$\bar{\Pi} = \frac{1}{2}\iiint_{\bar{V}} \left[\frac{1}{\mathrm{Bix}}\left(\frac{\partial\theta}{\partial\bar{x}}\right)^2 + \frac{L_x}{L_y}\frac{1}{\mathrm{Biy}}\left(\frac{\partial\theta}{\partial\bar{y}}\right)^2 + \frac{L_x}{L_z}\frac{1}{\mathrm{Biz}}\left(\frac{\partial\theta}{\partial\bar{z}}\right)^2\right] \cdot d\bar{V} - \iint_{\bar{S}_2}\bar{q}\theta d\bar{S} + \frac{1}{2}\iint_{\bar{S}_3}(\theta-1)^2 d\bar{S}, \quad (A.2)$$

where $\bar{\Pi} = \Pi/hT_\infty^2 L_yL_z$ is the dimensionless functional and $\bar{V} = V/(L_xL_yL_z)$ is the dimensionless volume whereas $\bar{S}_2 = S_2/(L_yL_z)$, and $\bar{S}_3 = S_3/(L_yL_z)$ are the dimensionless surface areas. Note that the functional is normalized with respect to L_yL_z, whereas the two alternate options are L_x L_z and L_xL_y which would provide similar expressions as equation (A.2), with different coefficients for $(\partial\theta/\partial\bar{x})^2$, $(\partial\theta/\partial\bar{y})^2$ and $(\partial\theta/\partial\bar{z})^2$ terms, also the definition of dimensionless surface areas would change accordingly.

The matrix form of the dimensionless functional is

$$\bar{\Pi} = \frac{1}{2}\iiint_{\bar{V}}\{\bar{\mathbf{g}}\}^T[\bar{\mathbf{D}}]\{\bar{\mathbf{g}}\}d\bar{V} - \iint_{\bar{S}_2}\{\boldsymbol{\theta}\}^T[\bar{\mathbf{N}}]^T\bar{q}d\bar{S} + \frac{1}{2}\iint_{\bar{S}_3}\left(\{\boldsymbol{\theta}\}^T[\bar{\mathbf{N}}]^T - 1\right)^2 d\bar{S}. \quad (A.3)$$

The dimensionless material property matrix $[\bar{\mathbf{D}}]$, shape function matrix $[\bar{\mathbf{N}}]$ and temperature gradient matrix $\{\bar{\mathbf{g}}\}$, are given by

$$[\bar{\mathbf{D}}] = \begin{bmatrix} \frac{1}{\mathrm{Bix}} & 0 & 0 \\ 0 & \left(\frac{L_x}{L_y}\right)\frac{1}{\mathrm{Biy}} & 0 \\ 0 & 0 & \left(\frac{L_x}{L_z}\right)\frac{1}{\mathrm{Biz}} \end{bmatrix},$$
$$\{\bar{\mathbf{g}}\} = [\bar{\mathbf{B}}]\{\boldsymbol{\theta}\}, \text{and } [\bar{\mathbf{B}}] = \left[\frac{\partial[\bar{\mathbf{N}}]}{\partial\bar{x}} \quad \frac{\partial[\bar{\mathbf{N}}]}{\partial\bar{y}} \quad \frac{\partial[\bar{\mathbf{N}}]}{\partial\bar{z}}\right]^T. \quad (A.4)$$

Putting $\{\bar{\mathbf{g}}\} = [\bar{\mathbf{B}}]\{\boldsymbol{\theta}\}$, gives

$$\bar{\Pi} = \{\boldsymbol{\theta}\}^T\left[\frac{1}{2}\iiint_{\bar{V}}[\bar{\mathbf{B}}]^T[\bar{\mathbf{D}}][\bar{\mathbf{B}}]d\bar{V}\right]\{\boldsymbol{\theta}\} - \{\boldsymbol{\theta}\}^T\iint_{\bar{S}_2}[\bar{\mathbf{N}}]^T\bar{q}d\bar{S} + \frac{1}{2}\iint_{\bar{S}_3}\left[\{\boldsymbol{\theta}\}^T[\bar{\mathbf{N}}]^T[\bar{\mathbf{N}}]\{\boldsymbol{\theta}\} - 2\{\boldsymbol{\theta}\}^T[\bar{\mathbf{N}}]^T + 1\right]dS \quad (A.5)$$

Minimizing the functional $\bar{\Pi}$ with respect to dimensionless temperature $\{\boldsymbol{\theta}\}$ gives

$$\left[\iiint_{\bar{V}}[\bar{\mathbf{B}}]^T[\bar{\mathbf{D}}][\bar{\mathbf{B}}]d\bar{V} + \iint_{\bar{S}_3}[\bar{\mathbf{N}}]^T[\bar{\mathbf{N}}]dS\right]\{\boldsymbol{\theta}\} = \iint_{\bar{S}_2}[\bar{\mathbf{N}}]^T\bar{q}d\bar{S} + \iint_{\bar{S}_3}[\bar{\mathbf{N}}]^T d\bar{S}. \quad (A.6)$$

The equation can be compared to the following standard finite element form to identify the stiffness and load matrices:

$$[\mathbf{k}]\{\boldsymbol{\theta}\} = \{\mathbf{f}\}. \tag{A.7}$$

Therefore, the element stiffness matrix is

$$\left[\bar{\mathbf{k}}\right] = \left[\bar{\mathbf{k}}_{\mathbf{q}}\right] + \left[\bar{\mathbf{k}}_{\mathbf{h}}\right], \tag{A.8}$$

with

$$\begin{aligned} \left[\bar{\mathbf{k}}_{\mathbf{q}}\right] &= \iiint_{\bar{V}} \left[\bar{\mathbf{B}}\right]^T \left[\bar{\mathbf{D}}\right] \left[\bar{\mathbf{B}}\right] d\bar{V}, \\ \left[\bar{\mathbf{k}}_{\mathbf{h}}\right] &= \iint_{\bar{S}_3} \left[\bar{\mathbf{N}}\right]^T \left[\bar{\mathbf{N}}\right] dS. \end{aligned} \tag{A.9}$$

Similarly, the load vector is

$$\left[\bar{\mathbf{f}}\right] = \left[\bar{\mathbf{f}}_{\mathbf{q}}\right] + \left[\bar{\mathbf{f}}_{\mathbf{h}}\right], \tag{A.10}$$

with

$$\begin{aligned} \left[\bar{\mathbf{f}}_{\mathbf{q}}\right] &= \iint_{\bar{S}_2} \left[\bar{\mathbf{N}}\right]^T \bar{q} d\bar{S}, \\ \left[\bar{\mathbf{f}}_{\mathbf{h}}\right] &= \iint_{\bar{S}_3} \left[\bar{\mathbf{N}}\right]^T d\bar{S}. \end{aligned} \tag{A.11}$$

The plane and axisymmetric cases can be directly deduced from the above generalized forms by adapting the $[\bar{\mathbf{B}}]$, $[\bar{\mathbf{D}}]$,$[\bar{\mathbf{N}}]$ and nondimensional element volume according to the two-dimensional problem type.

Data Availability

No underlying data was collected or produced in this study.

Disclosure

This study was performed as part of the employment of the authors at Texas A&M University Texarkana.

Conflicts of Interest

The author declares that they have no conflicts of interest.

References

[1] A. K. González, J. Rodríguez-Reséndiz, J. E. E. Gonzalez-Durán, J. M. Olivares Ramírez, and A. A. Estévez-Bén, "Development of a hip joint socket by finite-element-based analysis for mechanical assessment," *Bioengineering*, vol. 10, no. 2, p. 268, 2023.

[2] J. E. E. González-Durán, J. Rodríguez-Reséndiz, J. M. O. Ramirez, M. A. Zamora-Antuñano, and L. Lira-Cortes, "Finite-element simulation for thermal modeling of a cell in an adiabatic calorimeter," *Energies*, vol. 13, no. 9, p. 2300, 2020.

[3] J. E. E. Gonzalez Duran, O. J. González-Rodríguez, M. A. Zamora-Antuñano et al., "Finite element method and cut bar method-based comparison under 150°, 175° and 310° C for an aluminium bar," *Applied Sciences*, vol. 10, no. 1, p. 296, 2019.

[4] A. J. Baker, "Finite element solution algorithm for viscous incompressible fluid dynamics," *International Journal for Numerical Methods in Engineering*, vol. 6, no. 1, pp. 89–101, 1973.

[5] D. Winterscheidt and K. S. Surana, "p-version least-squares finite element formulation for convection-diffusion problems," *International Journal for Numerical Methods in Engineering*, vol. 36, no. 1, pp. 111–133, 1993.

[6] D. Winterscheidt and K. S. Surana, "P-version least squares finite element formulation for two-dimensional, incompressible fluid flow," *International Journal for Numerical Methods in Fluids*, vol. 18, no. 1, pp. 43–69, 1994.

[7] B. C. Bell and K. S. Surana, "p-version least squares finite element formulation for two-dimensional, incompressible, non-Newtonian isothermal and non-isothermal fluid flow," *International Journal for Numerical Methods in Fluids*, vol. 18, no. 2, pp. 127–162, 1994.

[8] N. B. Edgar and K. S. Surana, "*P*-version least squares finite element formulation for axisymmetric incompressible non-Newtonian fluid flow," *Computer Methods in Applied Mechanics and Engineering*, vol. 113, no. 3-4, pp. 271–300, 1994.

[9] C. S. Ling and K. S. Surana, "*P*-version least squares finite element formulation for axisymmetric heat conduction with temperature-dependent thermal conductivities," *Computers & Structures*, vol. 52, no. 2, pp. 353–364, 1994.

[10] L. C. Musson and K. S. Surana, "*P*-version least squares finite element formulation for three-dimensional, isothermal, Newtonian fluid flow," *Computers & Structures*, vol. 57, no. 1, pp. 107–124, 1995.

[11] Z. Feng and K. S. Surana, "*P*-version least squares finite element formulation for three-dimensional, isothermal, incompressible, non-Newtonian fluid flow," *Computers & Structures*, vol. 57, no. 5, pp. 799–816, 1995.

[12] H. S. Dalimunthe and K. S. Surana, "*P*-version least squares finite element formulation for three-dimensional, incompressible, non-isothermal, non-Newtonian fluid flow," *Computers & Structures*, vol. 58, no. 1, pp. 85–105, 1996.

[13] K. S. Vijayaraghavan and K. S. Surana, "*p*-version least-squares finite element formulation of a system of convection-reaction nonlinear equations-fixed bed *o*-xylene oxidation," *Computers & Structures*, vol. 62, no. 3, pp. 539–554, 1997.

[14] B. C. Bell and K. S. Surana, "A space–time coupled p-version least-squares finite element formulation for unsteady fluid dynamics problems," *International Journal for Numerical Methods in Engineering*, vol. 37, no. 20, pp. 3545–3569, 1994.

[15] B. C. Bell and K. S. Surana, "A space-time coupled p-version least squares finite element formulation for unsteady two-dimensional Navier–stokes equations," *International Journal for Numerical Methods in Engineering*, vol. 39, no. 15, pp. 2593–2618, 1996.

[16] D. Misra and A. Sarkar, "Finite element analysis of conjugate natural convection in a square enclosure with a conducting vertical wall," *Computer Methods in Applied Mechanics and Engineering*, vol. 141, no. 3-4, pp. 205–219, 1997.

[17] G. de Vahl Davis, I. P. Jones, and P. J. Roache, "'Natural convection in an enclosed cavity: a comparison problem', general announcement, e. g," *Computers and Fluids*, vol. 7, pp. 315-316, 1979.

[18] C. Taylor and A. Z. Ijam, "A finite element numerical solution of natural convection in enclosed cavities," *Computer Methods in Applied Mechanics and Engineering*, vol. 19, no. 3, pp. 429–446, 1979.

[19] J. N. Reddy and A. Satake, "A comparison of a penalty finite element model with the stream function-vorticity model of natural convection in enclosures," *Journal of Heat Transfer*, vol. 102, no. 4, pp. 659–666, 1980.

[20] W. N. R. Stevens, "Finite element, stream function–vorticity solution of steady laminar natural convection," *International Journal for Numerical Methods in Fluids*, vol. 2, no. 4, pp. 349–366, 1982.

[21] P. H. Oosthuizen, "The development of convective motion in a bottom heated square enclosure containing ice and water," *International Journal of Thermal Sciences*, vol. 40, no. 2, pp. 145–151, 2001.

[22] A. Barletta, E. Rossi di Schio, and E. Zanchini, "Combined forced and free flow in a vertical rectangular duct with prescribed wall heat flux," *International Journal of Heat and Fluid Flow*, vol. 24, no. 6, pp. 874–887, 2003.

[23] T. Basak, S. Roy, and A. R. Balakrishnan, "Effects of thermal boundary conditions on natural convection flows within a square cavity," *International Journal of Heat and Mass Transfer*, vol. 49, no. 23-24, pp. 4525–4535, 2006.

[24] E. Natarajan, S. Roy, and T. Basak, "Effect of various thermal boundary conditions on natural convection in a trapezoidal cavity with linearly heated side wall (s)," *Numerical Heat Transfer, Part B: Fundamentals*, vol. 52, no. 6, pp. 551–568, 2007.

[25] S. Roy, T. Basak, C. Thirumalesha, and C. M. Krishna, "Finite element simulation on natural convection flow in a triangular enclosure due to uniform and nonuniform bottom heating," *Journal of Heat Transfer*, vol. 130, no. 3, article 032501, 2008.

[26] M. Sathiyamoorthy, T. Basak, S. Roy, and I. Pop, "Steady natural convection flow in a square cavity filled with a porous medium for linearly heated side wall(s)," *International Journal of Heat and Mass Transfer*, vol. 50, no. 9-10, pp. 1892–1901, 2007.

[27] T. Basak, S. Roy, S. K. Babu, and I. Pop, "Finite element simulations of natural convection flow in an isosceles triangular enclosure filled with a porous medium: effects of various thermal boundary conditions," *International Journal of Heat and Mass Transfer*, vol. 51, no. 11-12, pp. 2733–2741, 2008.

[28] T. Basak, S. Roy, A. Singh, and I. Pop, "Finite element simulation of natural convection flow in a trapezoidal enclosure filled with porous medium due to uniform and non-uniform heating," *International Journal of Heat and Mass Transfer*, vol. 52, no. 1-2, pp. 70–78, 2009.

[29] M. M. Rahman, M. A. Alim, and M. A. H. Mamun, "Finite element analysis of mixed convection in a rectangular cavity with a heat-conducting horizontal circular cylinder," *Nonlinear Analysis: Modelling and Control*, vol. 14, no. 2, pp. 217–247, 2009.

[30] S. A. M. Mehryan, M. Ghalambaz, R. K. Feeoj, A. Hajjar, and M. Izadi, "Free convection in a trapezoidal enclosure divided by a flexible partition," *International Journal of Heat and Mass Transfer*, vol. 149, article 119186, 2020.

[31] I. A. Abbas, M. F. El-Amin, and A. Salama, "Effect of thermal dispersion on free convection in a fluid saturated porous medium," *International Journal of Heat and Fluid Flow*, vol. 30, no. 2, pp. 229–236, 2009.

[32] G. Palani and I. A. Abbas, "Free convection MHD flow with thermal radiation from an impulsively-started vertical plate," *Nonlinear Analysis: Modelling and Control*, vol. 14, no. 1, pp. 73–84, 2009.

[33] A. Rao, S. Sivaiah, and R. S. Raju, "Chemical reaction effects on an unsteady MHD free convection fluid flow past a semi-infinite vertical plate embedded in a porous medium with heat absorption," *Journal of Applied Fluid Mechanics*, vol. 5, no. 3, pp. 63–70, 2012.

[34] S. R. Sheri, A. J. Chamkha, and A. K. Suram, "Heat and mass transfer Effects on MHD Natural Convection Flow past an impulsively moving vertical plate with ramped temperature," *Journal of Applied Science and Engineering*, vol. 19, no. 4, pp. 385–392, 2016.

[35] M. D. Shamshuddin, O. Anwar Bég, M. Sunder Ram, and A. Kadir, "Finite element computation of multi-physical micropolar transport phenomena from an inclined moving plate in porous media," *Indian Journal of Physics*, vol. 92, no. 2, pp. 215–230, 2018.

[36] M. N. Dhaubhadel, J. N. Reddy, and D. P. Telionis, "Penalty finite-element analysis of coupled fluid flow and heat transfer for in-line bundle of cylinders in cross flow," *International Journal of Nonlinear Mechanics*, vol. 21, no. 5, pp. 361–373, 1986.

[37] C. A. J. Fletcher, "A primitive variable finite element formulation for inviscid, compressible flow," *Journal of Computational Physics*, vol. 33, no. 3, pp. 301–312, 1979.

[38] M. N. Dhaubhadel, J. N. Reddy, and D. P. Telionis, "Finite-element analysis of fluid flow and heat transfer for staggered bundles of cylinders in cross flow," *International Journal for Numerical Methods in Fluids*, vol. 7, no. 12, pp. 1325–1342, 1987.

[39] R. Mahmood, N. Kousar, K. Usman, and A. Mehmood, "Finite element simulations for stationary Bingham fluid flow past a circular cylinder," *Journal of the Brazilian Society of Mechanical Sciences and Engineering*, vol. 40, no. 9, pp. 1–9, 2018.

[40] M. A. Langthjem and Y. Sugiyama, "Dynamic stability of columns subjected to follower loads: a survey," *Journal of Sound and Vibration*, vol. 238, no. 5, pp. 809–851, 2000.

[41] C. D. Mote Jr., "Nonconservative stability by finite element," *Journal of the Engineering Mechanics Division*, vol. 97, pp. 645–656, 1971.

[42] R. S. Barsoum, "Finite element method applied to the problem of stability of a non- conservative system," *International Journal for Numerical Methods in Engineering*, vol. 3, no. 1, pp. 63–87, 1971.

[43] S. N. Prasad and G. Herrmann, "Adjoint variational methods in nonconservative stability problems," *International Journal of Solids and Structures*, vol. 8, no. 1, pp. 29–40, 1972.

[44] G. V. Rao and R. N. Rao, "Galerkin finite element solution for the stability of cantilever columns subjected to tangential loads," *AIAA Journal*, vol. 13, no. 5, pp. 690-691, 1975.

[45] G. V. Sankaran and G. Venkateswara Rao, "Stability of tapered cantilever columns subjected to follower forces," *Computers & Structures*, vol. 6, no. 3, pp. 217–220, 1976.

[46] B. N. Rao and G. Venkateswara Rao, "Stability of tapered cantilever columns subjected to a tip-concentrated follower force with or without damping," *Computers & Structures*, vol. 37, no. 3, pp. 333–342, 1990.

[47] G. V. Rao and P. C. Raju, "Post-buckling of uniform cantilever columns-Galerkin finite element solution," *Engineering Fracture Mechanics*, vol. 9, no. 1, pp. 1–4, 1977.

[48] B. J. Ryu and Y. Sugiyama, "Dynamic stability of cantilevered Timoshenko columns subjected to a rocket thrust," *Computers & Structures*, vol. 51, no. 4, pp. 331–335, 1994.

[49] B. J. Ryu, K. Katayama, and Y. Sugiyama, "Dynamic stability of Timoshenko columns subjected to subtangential forces," *Computers and Structures*, vol. 68, no. 5, pp. 499–512, 1998.

[50] M. A. Langthjem and Y. Sugiyama, "Optimum design of cantilevered columns under the combined action of conservative and nonconservative loads: part i: the undamped case," *Computers & Structures*, vol. 74, no. 4, pp. 385–398, 2000.

[51] M. A. Langthjem and Y. Sugiyama, "Optimum design of cantilevered columns under the combined action of conservative and nonconservative loads: part II: the damped case," *Computers & Structures*, vol. 74, no. 4, pp. 399–408, 2000.

[52] J.-S. Lee, N.-I. Kim, and M.-Y. Kim, "Sub-tangentially loaded and damped Beck's columns on two-parameter elastic foundation," *Journal of Sound and Vibration*, vol. 306, no. 3-5, pp. 766–789, 2007.

[53] M.-Y. Kim, J.-S. Lee, and M. M. Attard, "Stability of damped columns on a Winkler foundation under sub-tangential follower forces," *International Journal of Structural Stability and Dynamics*, vol. 13, no. 2, article 1350020, 2013.

[54] V. K. Goyal and R. K. Kapania, "A shear-deformable beam element for the analysis of laminated composites," *Finite Elements in Analysis and Design*, vol. 43, no. 6-7, pp. 463–477, 2007.

[55] V. K. Goyal and R. K. Kapania, "Dynamic stability of laminated beams subjected to nonconservative loading," *Thin-Walled Structures*, vol. 46, no. 12, pp. 1359–1369, 2008.

[56] E. Viola and A. Marzani, "Crack effect on dynamic stability of beams under conservative and nonconservative forces," *Engineering Fracture Mechanics*, vol. 71, no. 4-6, pp. 699–718, 2004.

[57] L.-W. Chen and K. Der-Ming, "Stability analysis of a Timoshenko beam subjected to distributed follower forces using finite elements," *Computers & Structures*, vol. 41, no. 4, pp. 813–819, 1991.

[58] J.-H. Kim and Y. S. Choo, "Dynamic stability of a free-free Timoshenko beam subjected to a pulsating follower force," *Journal of Sound and Vibration*, vol. 216, no. 4, pp. 623–636, 1998.

[59] L. Kwasniewski, "Numerical verification of post-critical Beck's column behavior," *International Journal of Nonlinear Mechanics*, vol. 45, no. 3, pp. 242–255, 2010.

[60] B. Sanz, J. Planas, V. Rey-de-Pedraza, R. Sancho, J. M. Sancho, and F. Gálvez, "Numerical and experimental study of initiation of cracking of UHPFRC by means of Brazilian tests," *Theoretical and Applied Fracture Mechanics*, vol. 118, article 103276, 2022.

[61] X. Fang and P. G. Charalambides, "The fracture mechanics of cantilever beams with an embedded sharp crack under end force loading," *Engineering Fracture Mechanics*, vol. 149, pp. 1–17, 2015.

[62] S. Bogdański and M. Trajer, "A dimensionless multi-size finite element model of a rolling contact fatigue crack," *Wear*, vol. 258, no. 7-8, pp. 1265–1272, 2005.

[63] S. Pashah, A. F. M. Arif, and S. M. Zubair, "Study of orthotropic pin fin performance through axisymmetric thermal non-dimensional finite element," *Applied Thermal Engineering*, vol. 31, no. 2-3, pp. 376–384, 2011.

[64] S. Pashah, A. F. M. Arif, and S. M. Zubair, "Efficiency of longitudinal composite fins with thermal Interface studied through plane thermal non-dimensional finite element," *Heat Transfer Engineering*, vol. 34, no. 7, pp. 629–641, 2013.

[65] S. Pashah, A. F. M. Arif, and S. M. Zubair, "Non-dimensional finite element formulation for thermal problems," in *ASME 2012 11th Biennial Conference on Engineering Systems Design and Analysis*, Nantes, France, 2012.

[66] S. Pashah, S. M. Zubair, and A. F. M. Arif, "Study of combined heat and mass transfer from fins using non-dimensional finite element formulation," in *ASME 2013 International Mechanical Engineering Congress and Exposition*, San Diego, California, USA, 2013.

[67] S. Pashah, S. M. Zubair, and A. F. M. Arif, "Study of coating effects on variable profile annular fins when subjected to dehumidifying operating conditions," *International Journal of Refrigeration*, vol. 48, pp. 60–70, 2014.

[68] N. Endahl, "On the finite element solution of the elastoplastic axisymmetric Hertz contact problem," *Computers & Structures*, vol. 24, no. 4, pp. 517–523, 1986.

[69] T. Basak, K. Kesava Rao, and A. Bejan, "A model for heat transfer in a honey bee swarm," *Chemical Engineering Science*, vol. 51, no. 3, pp. 387–400, 1996.

[70] P. Fredriksson and P. Gudmundson, "Size-dependent yield strength of thin films," *International Journal of Plasticity*, vol. 21, no. 9, pp. 1834–1854, 2005.

[71] I. A. Abbas and H. M. Youssef, "A nonlinear generalized thermoelasticity model of temperature-dependent materials using finite element method," *International Journal of Thermophysics*, vol. 33, no. 7, pp. 1302–1313, 2012.

[72] J. du Toit and C. Pretorius, "Steady-state heat transfer analysis in a spherical domain revisited," in *MATEC Web of Conferences*, vol. 347, p. 11, 12th South African Conference on Computational and Applied Mechanics (SACAM2020), 2021.

[73] R. W. Lewis, P. Nithiarasu, and K. N. Seetharamu, *Fundamentals of the Finite Element Method for Heat and Fluid Flow*, John Wiley & Sons, England, 2004.

[74] D. L. Logan, *A First Course in Finite Element Method*, Brooks/Cole, 3rd ed edition, 2002.

[75] A. E. Jeffers, "Heat transfer element for modeling the thermal response of non-uniformly heated plates," *Finite Elements in Analysis and Design*, vol. 63, pp. 62–68, 2013.

[76] ABAQUS, v., *6.10, Dassault Systemes Simulia Corporation*, Dassault Systemes Simulia Corporation, Providence, RI, 2010.

[77] ABAQUS, *6.11, Abaqus Analysis User's Manual, Section 31.15.1 User-defined elements*Dassault Systemes Simulia Corporation.

[78] ABAQUS, *6.11, Abaqus User Subroutines Reference Manual, Section 1.1.27 UEL*Dassault Systemes Simulia Corporation.

[79] L. Brouwer, D. Arbelaez, B. Auchmann, L. Bortot, and E. Stubberud, "User defined elements in ANSYS for 2D multiphysics modeling of superconducting magnets," *Superconductor Science and Technology*, vol. 32, no. 9, article 095011, 2019.

[80] ANSYShttps://www.ansys.com.

[81] H. M. Reeve, A. M. Mescher, and A. F. Emery, "Unsteady natural convection of air in a tall axisymmetric, nonisothermal annulus," *Numerical Heat Transfer, Part A: Applications*, vol. 45, no. 7, pp. 625–648, 2004.

[82] Fluent, Inc., *FIDAP User's Manual*, Fluent, Lebanon, NH, 1999.

[83] K. Khanafer and S. M. Aithal, "Laminar mixed convection flow and heat transfer characteristics in a lid driven cavity with a

circular cylinder," *International Journal of Heat and Mass Transfer*, vol. 66, pp. 200–209, 2013.

[84] ADINA, *Theory and Modeling Guide, vol. III: ADINA CFD & FSI, 2011*, pp. 265–278, ADINA R&D, Inc., Watertown, MA, 2012.

[85] ADINA, *Theory and Modeling Guide, vol. I: ADINA Solids & Structures (2012), Section 2.9.1: General elements and Section: 2.9.4 User supplied element*, ADINA R&D, Inc., 71 Elton Avenue Watertown, MA 02472 USA, 2012.

[86] H. E. Dillon, A. Emery, R. J. Cochran, and A. Mescher, "Dimensionless versus dimensional analysis in CFD and heat transfer," in *COMSOL Conference*, Boston, 2010.

[87] COMSOL, "Multiphysics," https://www.comsol.com.

[88] COMSOL Multiphysics Reference Manual, *Reference Manual, ver. 5.5, 2019. Section 16: equation-based modeling*, COMSOL, 2019.

[89] R. Bahadur and A. Bar-Cohen, "Orthotropic thermal conductivity effect on cylindrical pin fin heat transfer," *International Journal of Heat and Mass Transfer*, vol. 50, no. 5-6, pp. 1155–1162, 2007.

[90] S. M. Zubair, A. F. M. Arif, and M. H. Sharqawy, "Thermal analysis and optimization of orthotropic pin fins: a closed-form analytical solution," *Journal of Heat Transfer*, vol. 132, 2010.

[91] A. J. Baker, "A finite element solution algorithm for the Navier-stokes equations," No. NASA-CR-2391. NASA, 1974.